4

Effects of Gravity and Magnetic Field on Production of Single-Walled Carbon Nanotubes by Arc-Discharge Method

Tetsu Mieno and GuoDong Tan
Department of Physics, Shizuoka University
Japan

1. Introduction

Since the breakthrough enabling the mass production of single-walled carbon nanotubes (SWNTs) (Iijima 1993), many researchers in institutes and companies around the world have been developing efficient production methods for SWNTs (Harris, 1999). Various applications of this new and stable carbon nanomaterial with unique properties have been proposed (Jorio et al., 2008). However, insufficient control of the production of SWNTs is a major problem in developing applications of SWNTs. The mass production of long high-quality, defect-free SWNTs such as those with a length of 10 cm and a diameter of 1 nm is a major research target. Quality control in the production of SWNTs in terms of their diameter, chirality and defect density is also an important research target. Through the development of SWNTs, it is hoped that they can be used in strong and lightweight carbon wires and lightweight but strong composite bodies for many types of vehicles. Therefore, a basic study on the production process of SWNTs is very important for establishing new methods of producing high-quality SWNTs. In this study, the production of SWNTs by the arc discharge method is investigated. This is one of most popular methods of producing SWNTs, and it is essential to carry out the reaction in a hot helium gas atmosphere. As the reaction is strongly affected by gravity (heat convection) (Mieno, 2004) and the applied magnetic field (Lorentz force), the effects of gravity, heat convection and magnetic field on the production of SWNTs were experimentally studied. The process was examined under zero gravity, normal gravity and high gravity. As there are large differences among them, the authors discusses experimental results in comparison with reaction models and fluid simulation results. An investigation of the effect of applied magnetic field on inducing the JxB force in the arc plasma is also reported, and the effect of such a field on the production of SWNTs is clarified.

The effect of zero gravity was first examined using a vertical swing tower (VST), that repeatedly produces 1.1 s of zero gravity. Then, a series of parabolic-flight experiments were carried out with the support of Japan Space Forum, in which 10-20 periods of 20 s of zero gravity were obtained per flight. The results were compared with those of the laboratory experiment. A higher-gravity experiment was carried out using a rotating acceleration generator, which produces gravity of 1-3 g_0 (g_0: normal gravitational acceleration). The produced SWNTs were measured by TEM, Raman spectrometry and other methods.

2. Theoretical model of production process under selected reaction conditions

Figure 1 shows a reaction model of SWNTs fabricated by the arc-discharge method. Sublimated carbon molecules and metal atoms diffuse in the region of hot He gas, where the metal atoms fuse to form nanosize catalytic particles, and carbon atoms diffuse into the catalyst particles or diffuse on them. During the cooling process of the hot gas, SWNTs grow on the catalyst particles, which is a self-organizing process, and no special mould is used. The reaction is strongly affected by the gas temperature, the diffusion speed, the cooling rate of the particles, the carbon density and the catalyst particle density.

When spherical carbon clusters of the same diameter and mass are produced in a globe, which is located at the centre of spherical coordinates and has radius of r_0, and the clusters diffuse continuously and isotropically with diffusion coefficient D_C without any external forces or chemical reactions, the density profile of the carbon clusters $n_C(r)$ and radial cluster flux J_C (r) can be calculated by Fick's diffusion laws (Cussler, 1984; Mieno & Takeguchi, 2006). Under the steady flow condition,

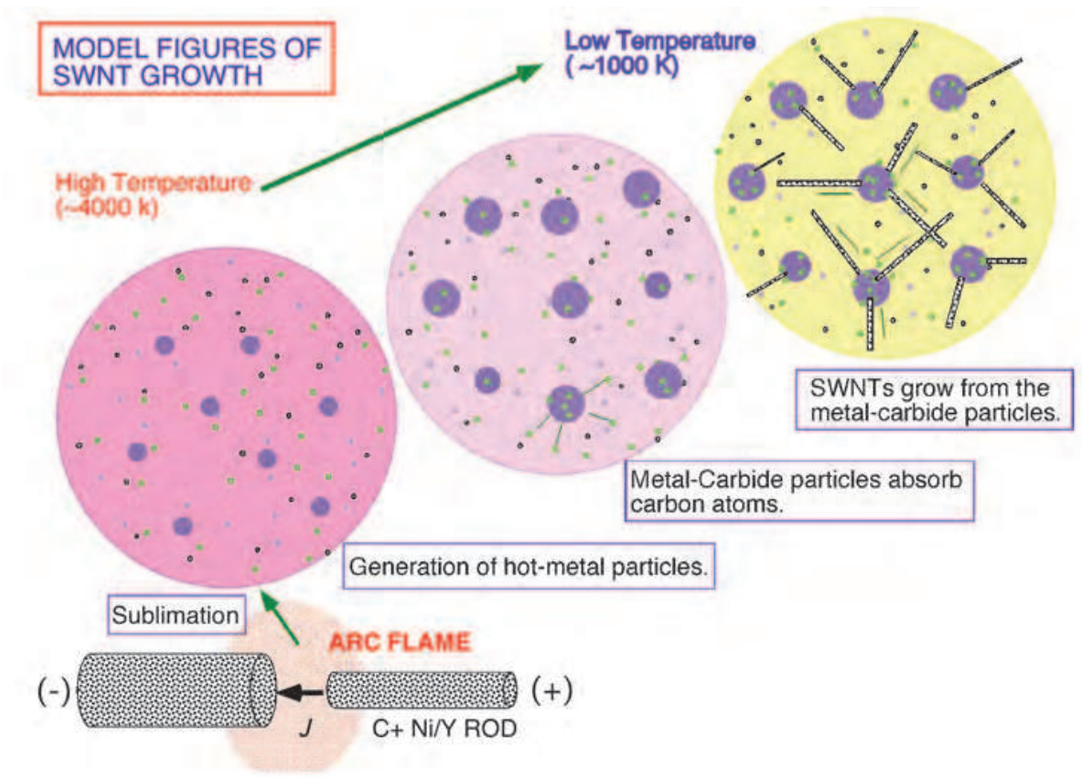

Fig. 1. Model of production process of SWNTs in He gas phase fabricated by the arc discharge method, in which metal catalyst particles play an important role.

$$n_C(r) = \frac{r_1 r_0}{r_1 - r_0}(n_0 - n_1)\frac{1}{r} + \frac{r_1 n_1 - r_0 n_0}{r_1 - r_0} \tag{1}$$

$$J_C(r) = D_C \frac{r_1 r_0}{r_1 - r_0}(n_0 - n_1)\frac{1}{r^2} \tag{2}$$

where $r_1 > r > r_0$. n_0 and n_1 are the cluster densities at $r = 0$ and $r = r_1$, respectively. When the carbon clusters diffuse in a noble gas, according to classical diffusion theory (Bird et al., 1960; Mieno, 2006) their diffusion coefficient D_{CN} is written as

$$D_{CN} = \frac{4}{3}\frac{\sqrt{2}}{\pi^{3/2}}\left(\frac{1}{m_C}+\frac{1}{m_N}\right)\frac{(\kappa_B T)^{3/2}}{p(d_C+d_N)^2} \tag{3}$$

where m_C and m_N are the cluster mass and noble atom mass, respectively. l_B, T, p, d_C and d_N are Boltzmann's constant, the gas temperature, the gas pressure, and the diameters of the cluster and noble-gas atom, respectively. From these equations, the ideal radial diffusion velocities of the clusters can be calculated. Figure 2 shows the thermal diffusion velocities of carbon clusters C_2, C_{60}, C_{1000} and C_{10000} as a function of He gas pressure, where the clusters are assumed to be spherical, the He temperature is $T = 5000$ K and $r = 3.0$ cm from the centre (the centre of the arc flame). These boundary conditions are based on the experimental cylindrical vessel (102 mm in diameter and 184 mm high).

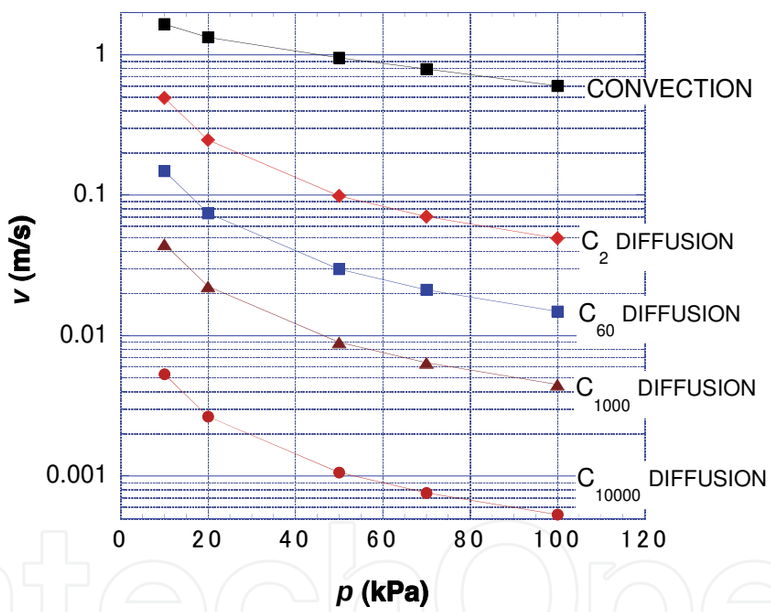

Fig. 2. He pressure dependence of thermal diffusion velocities of carbon clusters and helium convection velocity. Calculation at $T = 5000$ K.

Under the normal gravity, the gravitational force causes strong heat convection, in which all the carbon clusters flow upward with the He gas under a collisional pressure condition. This convection velocity can be calculated using a set of fluid equations. Here, a simulation by the simplified marker and cell (SMAC) method (Payret & Taylor, 1983) (Mizuho Information & Research Institution Inc., Fuji-RIC/Alfa-Flow) was used. The heat convection velocity versus He gas pressure under normal gravity is shown in figure 2. The heat convection velocity is much larger than the diffusion velocity of the clusters. Therefore, it can be expected that under zero gravity, the diffusion velocity of the clusters dramatically decreases. From equation 3, it is expected that larger and heavier clusters diffuse more

slowly in He gas. In the case of SWNTs, the structure is chainlike, which decreases their mobility in the gas. From the measurement of the mobilities of fullerenes, chainlike carbon clusters and ring-type carbon clusters, it was shown that the diffusion velocity of long-chain-type clusters is about half that of spherical clusters with the same mass (von Helden et al., 1993). Therefore, SWNTs are estimated to have half the diffusion velocity of spherical carbon clusters with the same mass. In the case of arc discharge, carbon atoms diffuse from the arc-plasma region. Therefore, this large suppression of the diffusion speed under zero-gravity should realize high-temperature long-time hot reaction for synthesizing SWNTs.

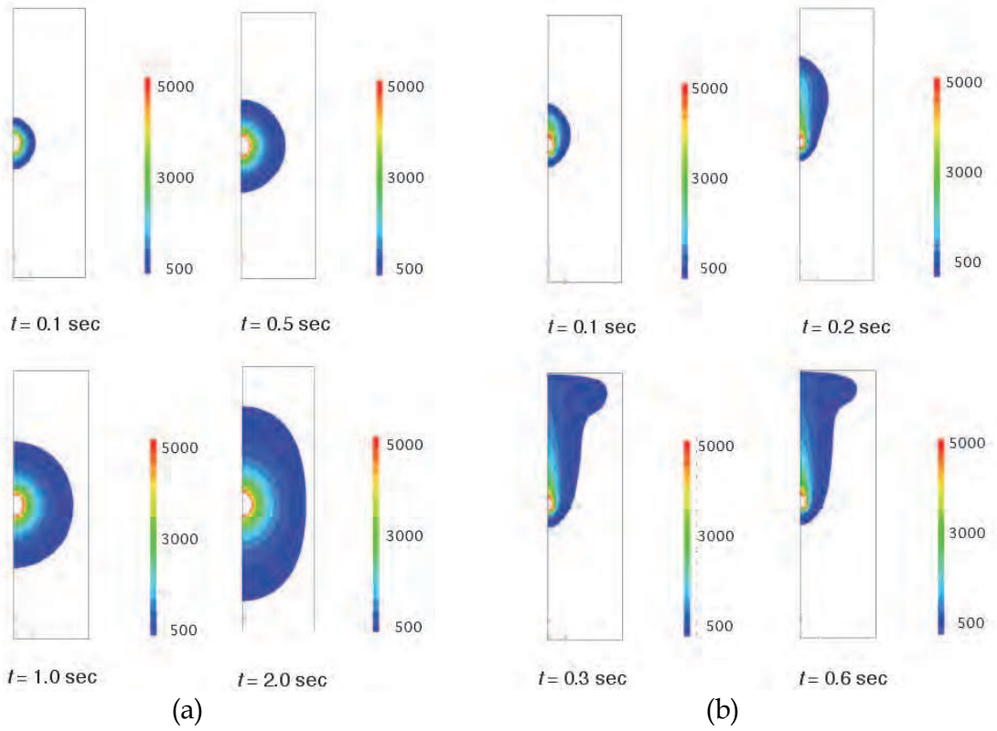

Fig. 3. Simulation results of temperature contours (T= 500-5000 K). (a) zero gravity, (b) normal gravity. p(He)= 40 kPa, and the arc starts at t= 0.

If the heat convection is suppressed, the gas atoms and clusters isotropically diffuse, resulting in the high-temperature gas region around the arc plasma becoming spherical and the volume of this region becoming much larger. Using the SMAC simulation method, the time evolution of the He gas temperature contours around the plasma was calculated and is shown in figures 3(a) and 3(b) (Mieno, 2006). These figures show the profiles of He gas temperature contours under (a) zero gravity and (b) normal gravity, and the right half of the reaction chamber is visualized. Here, p(He)= 40 kPa, the input electric power is P_{IN}= 1.0 kW and T= 500-5000 K. Under zero gravity, the temperature contours isotropically and monotonically expand until the contour arrives at the side wall (t~ 2 s). It takes more than 1 min for the temperature distribution to reach a steady-state condition. In contrast, under normal gravity, the contours expand only in the upward direction and attain a steady-state condition within 0.6 s. Thereafter, the temperature contours exhibit almost no change with

time, which means that the produced thermal energy is continuously transported to the upper wall under this condition.

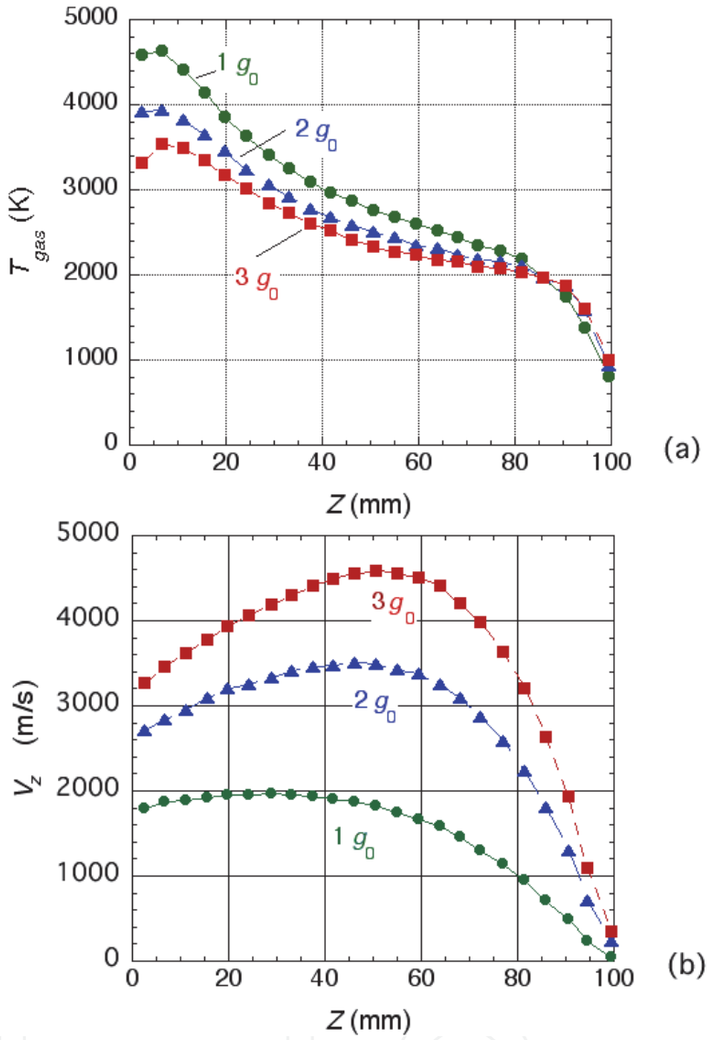

Fig. 4. (a) Vertical (z) direction distributions of gas temperatures for gravitational strengths of 1.0 g_0, 2.0 g_0 and 3.0 g_0, where the centre of the arc flame is set to z= 0 cm. r= 1.1 cm, p(He)= 50 kPa and P_{IN}= 1.0 kW. (b) vertical direction distributions of gas velocity V_z for the three gravitational strengths.

When the gravity is increased from 1.0 g_0 to 3.0 g_0, the temperature contours and gas velocities exhibit distinct properties. Using the SMAC simulation method, the temperature contours were calculated (Tan & Mieno, 2010b). The vertical distributions of the gas temperature along the z direction at r= 1.1 cm for three gravitational strengths are graphed as shown in figure 4(a), where p(He) = 50 kPa and P_{IN}=1.0 kW. The corresponding vertical distributions of the gas velocity V_z were calculated and are shown in figure 4(b). The gas temperature above the plasma decreases with increasing gravity. Whereas V_z above the plasma increases with increasing gravity. From these calculations, the vertical distribution of the gas cooling rate can be evaluated. The results for the three gravity conditions

corresponding to figures 4(a) and (b) are shown in figure 5. At around z= 20 mm, the highest cooling rate is observed for these gravities. Increasing gravity (3 g_0) increases this cooling rate at z= 20 - 80 mm. These simulation results are easily explained by the simple fluid model.
When a steady-state magnetic field is applied to the arc plasma, electrons and ions are accelerated by the Lorentz force (F= JxB**)** as shown in figure 6. At first, electrons are accelerated in the JxB direction, and then ions are accelerated in the same direction by an ambipolar electric field. By the Lorentz force, the plasma and neutral particles including many carbon atoms and metallic atoms are jetted out in the JxB direction, and sublimated carbon atoms are efficiently transformed from the electrode region, by which the redeposition of carbons in the gas phase to the cathode is supressed (Aoyama & Mieno, 1999), and thus an efficient reaction to produce SWNTs is expected.

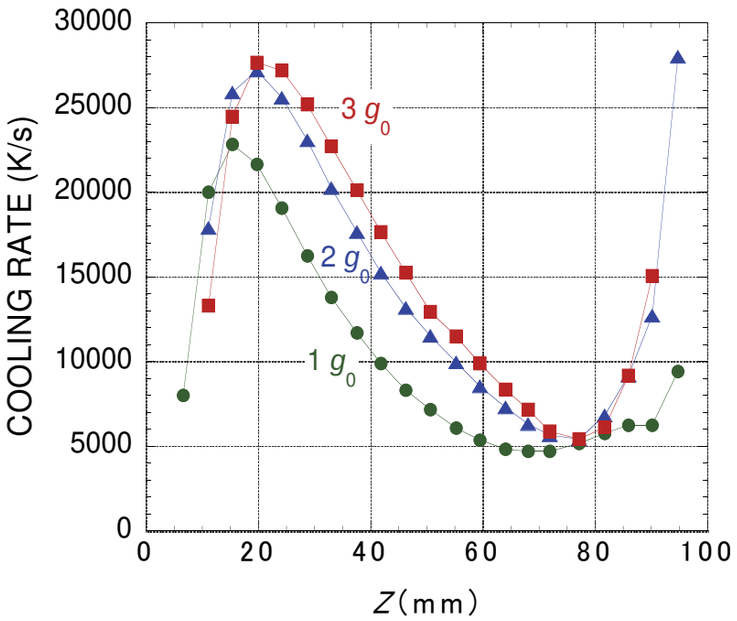

Fig. 5. Vertical distributions of calculated cooling rates of the gas for the three gravitational strengths. p(He)= 50 kPa and P_{IN}= 1.0 kW.

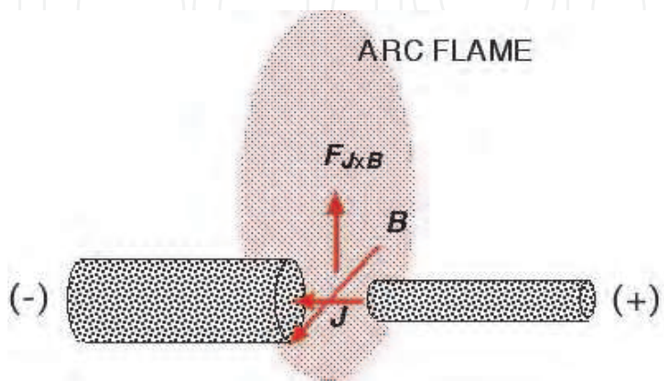

Fig. 6. Model figure of the JxB arc discharge.

3. Production of SWNTs by arc-discharge method

3.1 Gravity-free production by means of parabolic flight

At first, we constructed a 12-m-high vertical swing tower (VST) in the university campus supported by the Institute of Space & Astronautical Science, Japan (ISAS/JAXA). A photograph and the schematic of the VST are shown in figure 7. Suspended by a thin stainless wire and a 2-m-long rubber rope, an arc reactor was swung by force from an air cylinder, and a constant-amplitude swing of the reactor was realized (Mieno, 2004). The amplitude is about 4 m peak to peak, the period was 2.3 s and the gravity-free time was 1.1 s. Synchronous with this swing, the arc-discharge current was pulse-time-modulated. After about 30 min of swinging, 15 min of integrated gravity-free production was realized. By this method, SWNTs were produced (Kanai et al., 2001). The result shows that amount of produced carbon soot increased by about 13.5 times that produced under normal gravity. However, 1.1 s of gravity-free time was not sufficient to form a large and spherical gas region for synthesizing SWNTs.

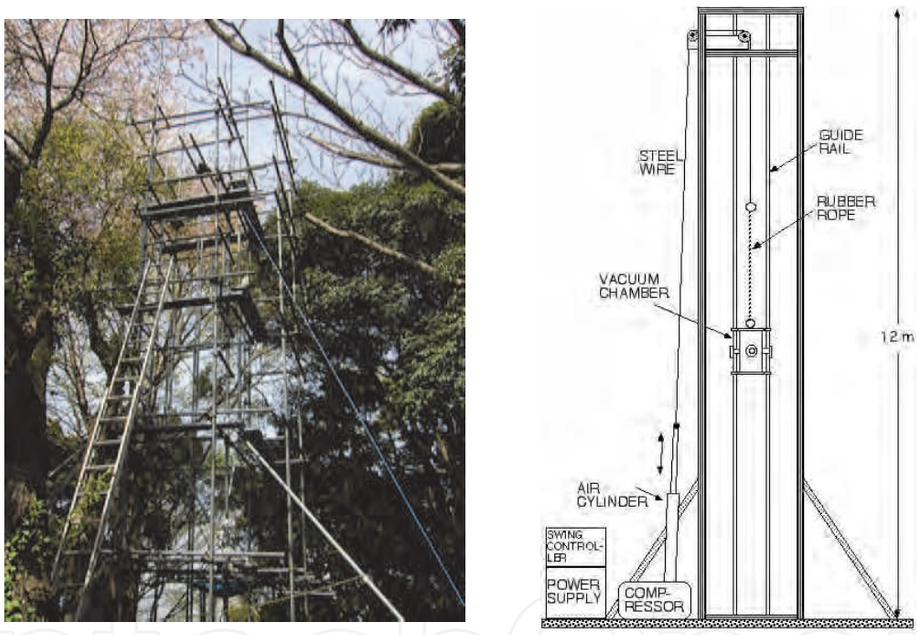

Fig. 7. Photograph and schematic of 12-m-high vertical swing tower (VST).

Then, I had the chance to perform an experiment using a specially prepared jet plane in Japan, in which a repetitive series of experiments under 20 s of microgravity condition was conducted using parabolic flights. I tried to examine the microgravity effects in the production of SWNTs by this method (Mieno, 2006, Mieno & Takeguchi, 2006). We developed special equipment for this purpose (which includes a small arc reactor, a DC power supply, a pumping system, a gas-feeding system, diagnostic systems such as video cameras, thermocouples, and a Mie scattering unit.) as shown in figure 8. The equipment was installed in the jet plane (Grumman G-II), which was operated to make repeated parabolic flights (Mieno, 2003). In one flight, 10-20 parabolic flights were carried out, by which 200-400 s of the integrated gravity-free production of SWNTs were realized. The reactor is a cylindrical metal chamber 16 cm in diameter and 20 cm high, in which a carbon rod anode 6.0 mm in diameter including Ni/Y metal particles and a carbon rod cathode 10.0 mm in diameter were set.

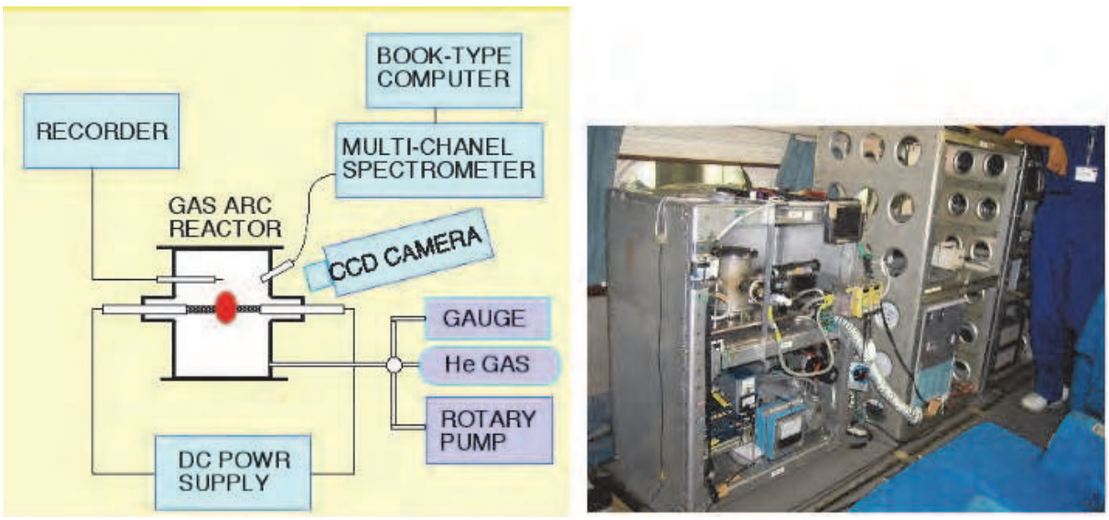

Fig. 8. Schematic and photograph of the reactor installed in the jet plane.

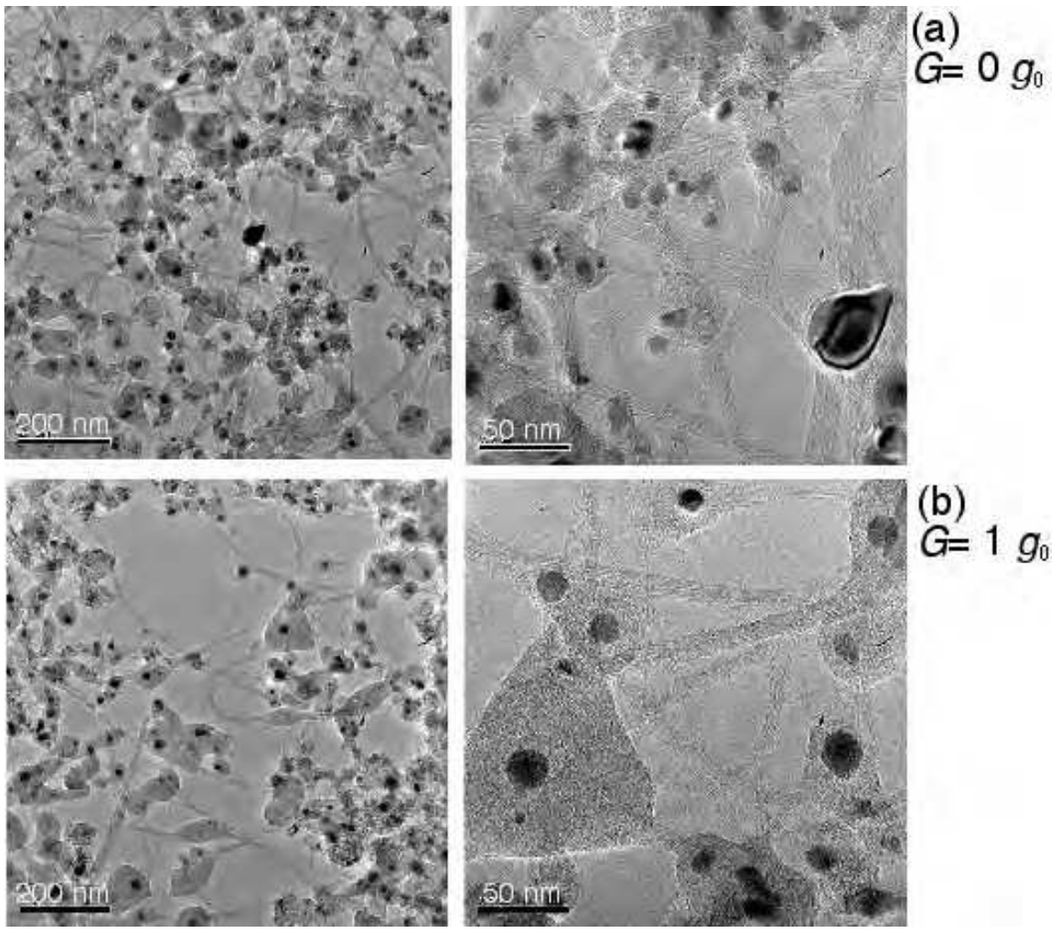

Fig. 9. Typical TEM images of SWNTs produced under two gravity conditions. p(He)= 65 kPa, I_d~ 50 A.

After evacuating the reactor with a rotary pump, He gas was introduced in the reactor and the reactor was closed. A DC power supply (Daihen Co., VRTP-200) was used to continue DC arc discharge under a constant current.

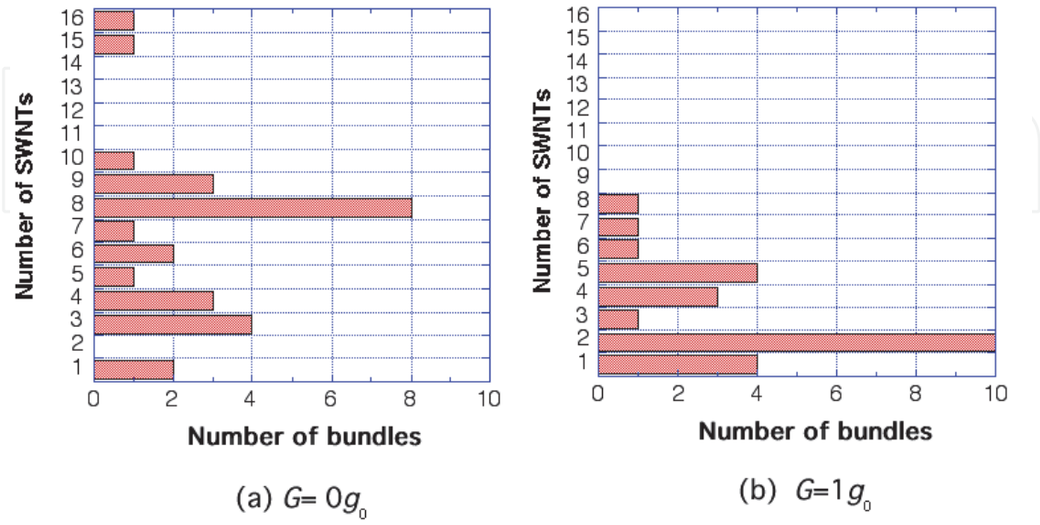

Fig. 10. Number of observable SWNTs in a bundle counted from figure 9. Shaded SWNTs in each bundle are not counted.

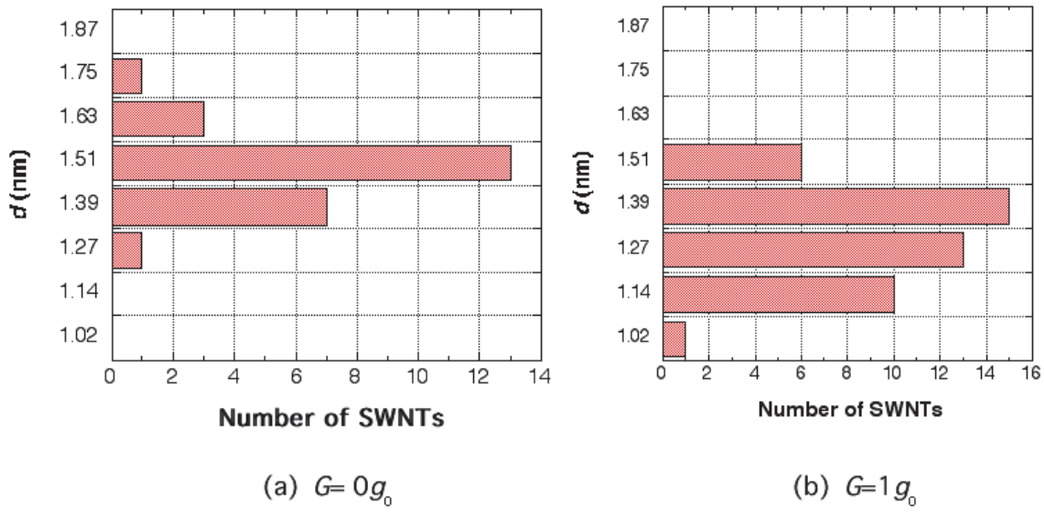

Fig. 11. Diameter distributions of SWNTs in figure 9.

To clarify the gravity effect, the production was carried out on the ground under the same discharge condition of zero gravity. After the production, the produced carbon soot was carefully collected and analysed. The TEM images of the produced SWNTs are shown in Fig. 9, where p(He)= 65 kPa and discharge current I_d= 50 A. Under zero gravity, thicker bundles of SWNTs with higher content were produced than those under normal gravity. The diameter is about 1.5 nm. From the TEM images, the number of observable SWNTs in a bundle was measured, and its histograms are shown in figure 10. From this figure it was

confirmed that thicker bundles of SWNTs were produced under zero gravity. Also the diameter distribution of SWNTs in figure 9 was measured, and its histograms are shown in figure 11. Under zero gravity, thicker SWNTs (average diameter of 1.5 nm) were produced. For the gravity-free experiment, the main target is production of much longer SWNTs. Although the SWNTs shown in figure 9(a) appear to be more than 100 nm, longer than those produced under the normal gravity, it is difficult to confirm the length of each nanotube. The length of most of the SWNTs did not exceed 1 mm. It is conjectured that 20 s of gravity-free time is not enough to produce very long SWNTs. Further analysis and a search for better methods are now under way.

3.2 High-gravity production using rotating acceleration generator

To clarify the gravity effects, SWNTs were produced under high gravity. In this case, stronger heat convection is expected and the reactor time decreases. For this purpose, the rotating acceleration generator of JAXA, Japan was used.

The photograph of the generator is shown in figure 12. The generator has a 6.5-m-long arm rotating at a constant speed to reach an acceleration of 0 – 490 m/s^2. (Tan & Mieno, 2010a) On one end of the arm, the experimental set up was installed, and by remote control with a motor drive and video cameras, arc discharge under a continuous high gravity was carried out. Under 2-g_0 and 3-g_0, stronger heat convections were clearly observed by the passive Mie scattering method, in which direct light from the arc plasma was cut by a metal plate, and scattered lights from the clusters are recorded. (Mieno, 2006b) Figure 13(a) shows a Mie scattering image under 3 g_0 (side view), in which the white clouds are carbon clusters flowing from the plasma region forming one large swirl, where p(He)= 50 kPa, I_d= 40 A and t= 4.0 min. Figure 13(b) shows corresponding velocity distribution calculated by the SMAC method. A large swirl (cluster flow) from the inner side to the outer side is clearly obtained. After the experiment, the produced soot was carefully collected and analysed by Raman spectrometry and TEM. Figure 14 shows the produced soot yield versus applied gravity G, where p= 50 kPa and I_d= 50 A. During the discharge, the discharge voltage was stable and should little change with gravity. However, the soot yield gradually increased with gravity.

Fig. 12. Photograph of the rotation acceleration generator of JAXA.

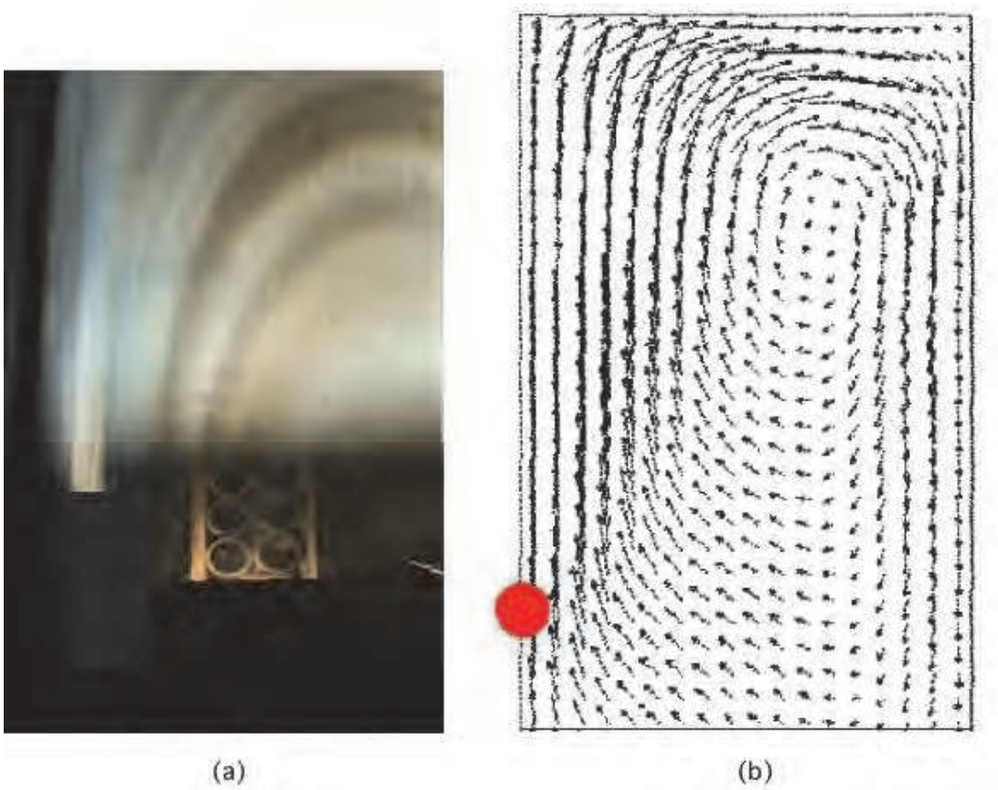

Fig. 13. (a) Mie scattering image of the carbon-cluster flow from the plasma region under 3 g_0 (side view). p(He)= 50kPa, I_d= 40 A, t= 4.0 min. (b) Corresponding calculation of the gas velocity by the SMAC method.

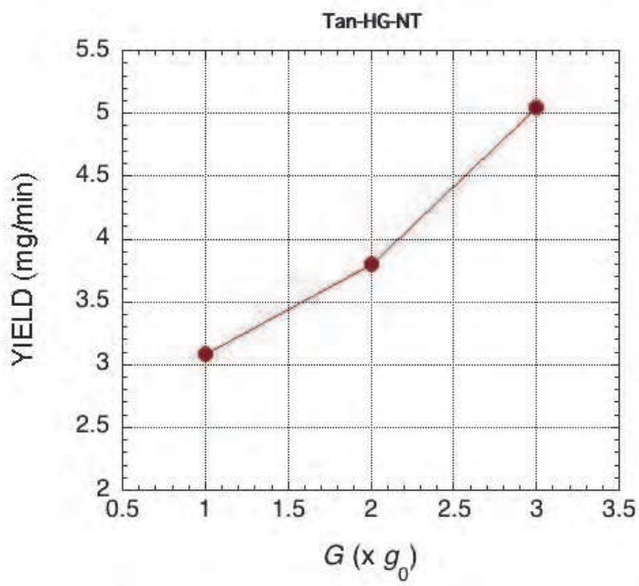

Fig. 14. Yield of carbon soot versus applied gravity G. p(He)= 50 kPa and I_d= 50 A.

To determine the production site of SWNTs, a cylindrical carbon collector array (each cylinder is 0.8 cm in diameter and 2.0 cm long) was installed 1.0 cm from the arc centre (Tan & Mieno, 2010a). The soot is collected at z= 0, 10, 20, 30, 40, 50, 60, 70 and 80 mm. The Raman spectra of the collected soot at 5 vertical positions under 1 g_0 are shown in figure 15,

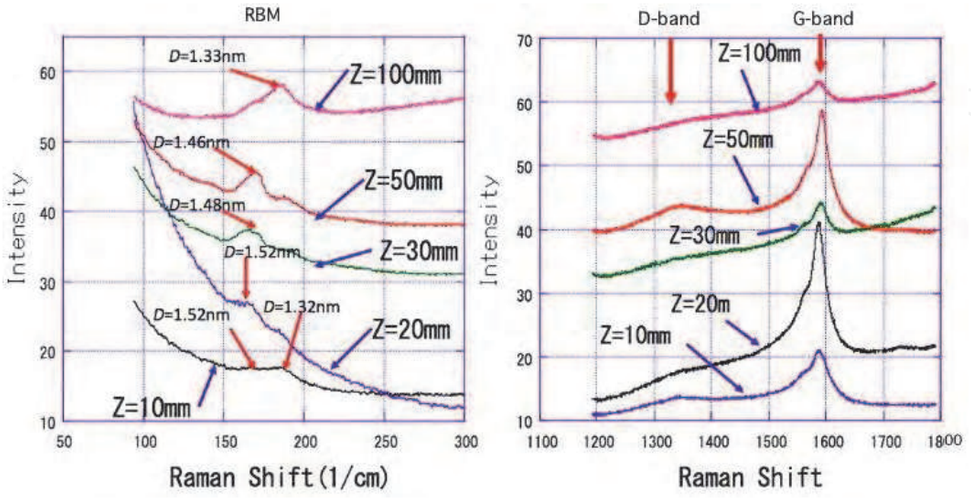

Fig. 15. Raman spectra of the soot produced under 1.0 g_0. The RBM, G-band and D band of soot collected at five positions are shown.

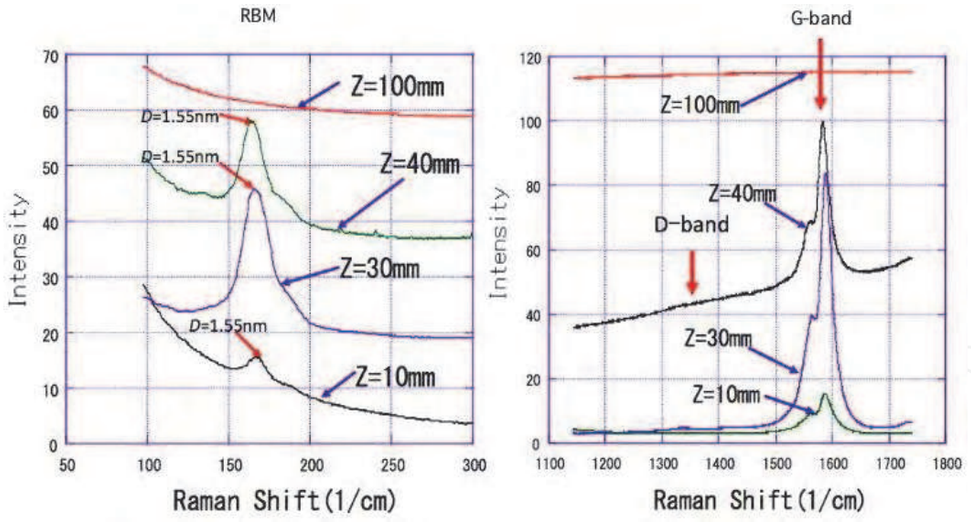

Fig. 16. Raman spectra of the soot produced under 3.0 g_0. The RBM, G-band and D band of soot collected at several positions are shown.

where the radial breathing modes (RBM) of SWNTs are shown on the left side. The G-band and D-band of carbon are shown on the right side. Vertical direction variations of these signals can be confirmed. In the same way, the Raman spectra of the carbon soot under 3 g_0 are shown in figure 16. Under this condition, the RBM and G-band are clearly obtained only at z= 10, 30 and 40 mm. At higher positions, no clear peaks from SWNTs were obtained. As expected from the theory, the higher the gravity, the higher convection speed, which

reduces the reaction time for producing SWNTs in a hot gas atmosphere. This model supports the results shown by the Raman spectra in figures 15 and 16.
From the Raman spectra, the vertical distributions of G/D ratio for the soot produced under the three gravitational conditions were evaluated and are shown in figure 17 (Tan & Mieno, 2010a). This G/D ratio indicates the relative content of SWNTs in the produced soot, because the disordered carbon impurity emits the D-band signal. We can find that the G/D ratios under 3 g_0 at z= 10, 20 and 30 mm are much higher than those under 1 g_0, in spite of the stronger heat convection. This phenomenon can be explained from the model calculation. From the Mie scattering image and calculation in figure 13, it can be conjectured that the large swirl observed in the chamber flows down the carbon particles from the top wall region to the hot gas region, which makes the repetitive heating of carbon particles crucial for producing good SWNTs.

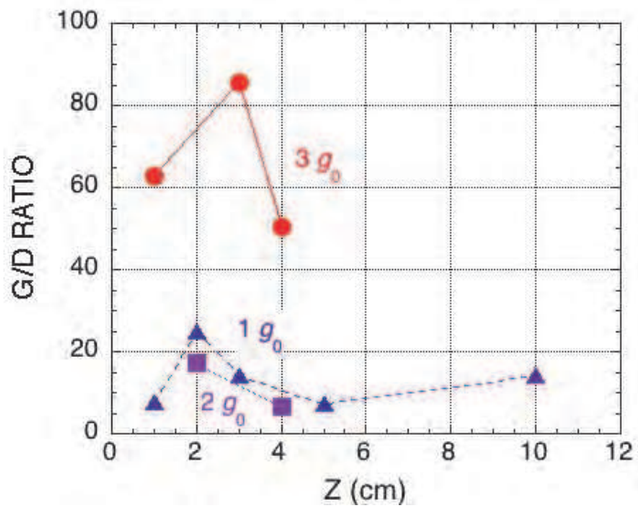

Fig. 17. Vertical distributions of G/D ratio for the soot produced under the three gravitational conditions.

3.3 Production under steady-state magnetic field

After considering the control of gas flow around the arc plasma, it was found that a steady-state magnetic field applies a JxB force to the plasma and changes the flow of sublimated carbon molecules (Aoyama & Mieno, 1999). The plasma flow affected by the magnetic field can be observed from a viewing port of the arc reactor, as shown in figure 18 (Matsumoto & Mieno, 2003). A strong upper flow of the plasma along the JxB direction was clearly observed (figure 18 (b)). To confirm this effect, an arc discharge experiment with a magnetic field was carried out (Mieno et al., 2006). Depending on the field, the production rate of the soot including SWNTs increased, as shown in figure 19, where p(He)= 60 kPa and I_d= 50 A. By the Raman spectrometry and TEM, the characteristics of produced SWNTs are determined (Mieno et al., 2006). The Raman spectra of the soot including SWNTs under the two magnetic fields are shown in figure 20, where p(He)= 60 kPa and I_d= 50 A. From the RBMs in the left graphs, the diameter of SWNTs, d, can be estimated and is written on the top of the figure. By applying the magnetic field, the diameter distribution is narrower and the main diameter is 1.4 nm. In the right graphs, the peaks of the G-band and D-band of carbon are shown. A good G/D ratio was obtained and the D-band signal was very small with application of a magnetic field.

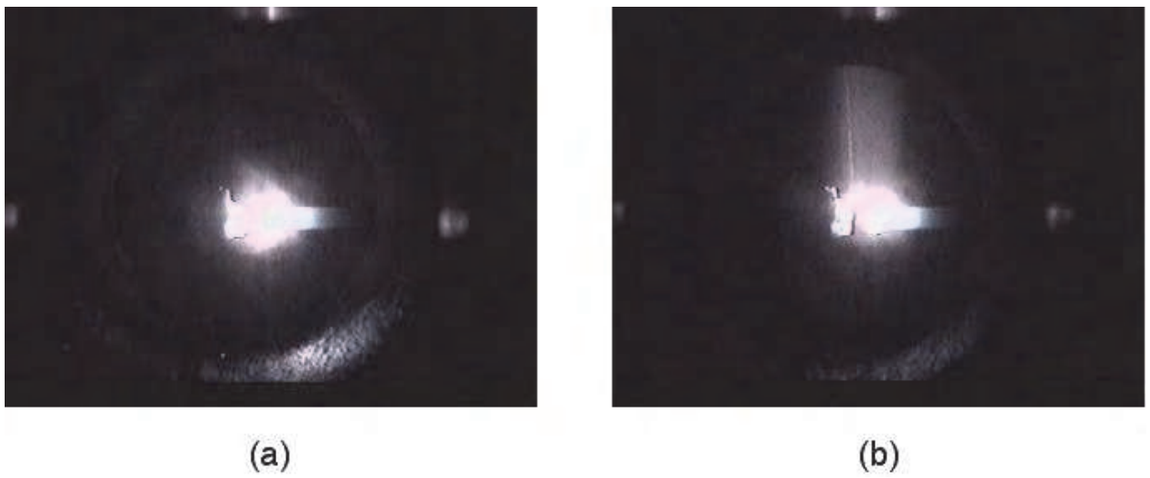

Fig. 18. Typical images (side views) of the arc flame. (a) No magnetic field and (b) *J*x*B* arc discharge.

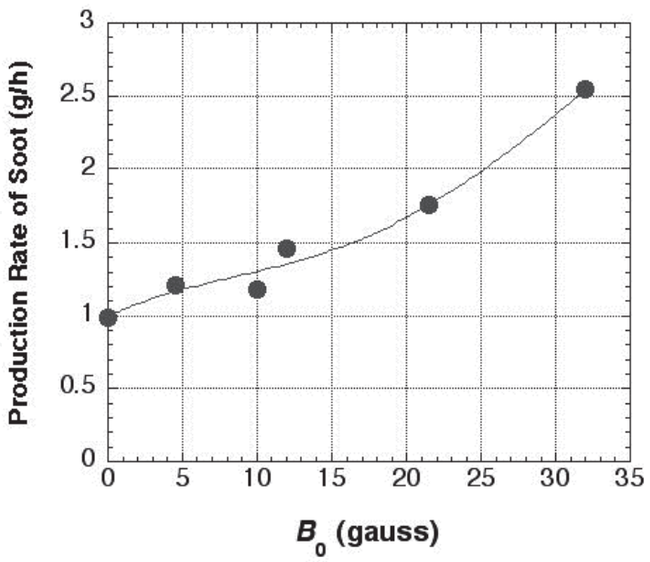

Fig. 19. Production rate of soot icluding SWNTs vs applied magnetic field.

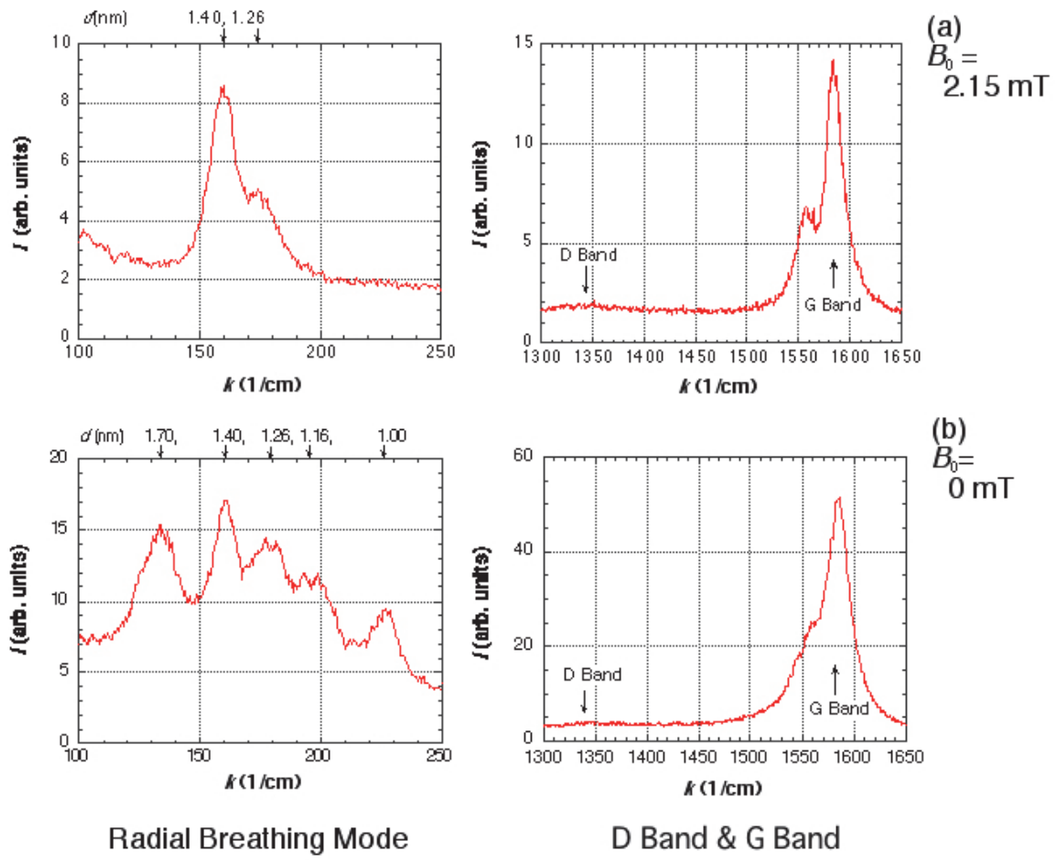

Fig. 20. Raman spectra of the soot including SWNTs under the two magnetic fields. p(He)= 60 kPa and I_d= 50 A. From the RBMs in the left graphs, the diameter of SWNTs, d, can be estimated and is written on the top of the figure. In the right graphs, the peaks of the G-band and D-band of carbon are shown.

3. Conclusion

Control of the reaction conditions in the hot gas phase is important for the production of high-quality SWNTs, because the analysis and control of the production process of SWNTs have not yet been investigated. Now, to improve the production of longer and high-quality SWNTs, a basic study of the production process is necessary. Here, the effects of zero-gravity, high-gravity and the JxB arc jet condition for the production of SWNTs were investigated. Under the zero-gravity and the JxB arc jet condition, considerably excellent production was obtained. However, the mass production of long SWNTs (more than 1 cm) could not be achieved. Therefore, further experimental and simulation studies are necessary. This challenge would lead to breakthroughs in the worldwide use of SWNTs.

4. Acknowledgments

I would like to thank Mr. N. Matsumoto for his collaboration as a graduate student. This study was partly supported by Japan Space Forum (JSF), ISAS/JAXA and The Ministry of Education, Culture, Sports, Science &Technology (MEXT), Japan.

5. References

Aoyama, A. & Mieno, T. (1999) Effect of Gravity and Magnetic Field in Production of C_{60} by a DC Arc Discharge, *Japanese Journal of Applied Physics*, Vol. 38, No. 3A, pp. L267-L269

Bird, R. B. et al. (1960). Transport Phenomena, Wiley, New York, p. 337

Cussler, E. L. (1984). Diffusion: Mass Transfer in Fluid Systems, Cambridge University Press, New York, p. 19

Harris, P. J. F. (1999). Carbon Nanotubes and Related Structures, Cambridge University Press, ISBN 0-521-00533-7, Cambridge

Iijima, S. (1993). Single-Shell Carbon Nanotubes of 1-nm Diameter, *Nature*, Vol. 363, pp. 603-605

Jorio, A. et al. (eds.) (2008). Carbon Nanotubes, Springer-Verlag, ISBN 978-3-540-72864-1, Berlin

Kanai, M. et al. (2001). High-yield synthesis of single-walled carbon nanotubes by gravity-free arc discharge, *Applied Physics Letters*, Vol. 79, No. 18, pp. 2967-2969

Matsumoto, N. & Mieno, T. (2003). Characteristics of heat flux of *JxB* gas-arc discharge for the production of fullerenes, *VACUUM*, Vol. 69, pp. 557-562

Mieno, T. (2003). Gas Temperature Evolution of the Gravity-Free Gas Arc Dicharge under a Parabolic Flight of Jet Plane, *Japanese Journal of Applied Physics*, Vol. 42, No. 8A, pp. L960-L963

Mieno, T. (2004). Characteristics of the gravity-free gas-arc discharge and its application to fullerene production, *Plasma Physics and Controlled Fusion*, Vol. 46, pp. 211-219

Mieno, T. & Takeguchi, M. (2006). Thermal motion of carbon clusters and production of carbon nanotubes by gravity-free arc discharge, *Journal of Applied Physics*, Vol. 99, pp. 104301-1-5

Mieno, T. (2006). Diffusion and Reaction of Carbon Clusters in Gas Phase for Production of Carbon Nanotubes, *New Diamond and Frontier Carbon Technology*, Vol. 16, No. 3, pp. 139-150

Mieno, T.; Matsumoto N. & Takeguchi, M. (2006). Efficient Production of Single-Walled Carbon Nanotubes by *JxB* Gas-Arc Method. *Japanese Journal of Applied Physics*, Vol. 43, No. 12A, pp. L1527-1529

Payret, R. & Taylor, T. D. (1983). Computational Methods for Fluid Flow, Springer, New York, p. 160

Tan, G. & Mieno, T. (2010a). Synthesis of single-walled carbon nanotubes by arc-vaporisation under high gravity condition, *Thin Solid Films*, Vol. 518, pp. 3541-3545

Tan, G. & Mieno, T. (2010b). Experimental and Numerical Studies of Heat Convection in the Synthesis of Single-Walled Carbon Nanotubes by Arc Vaporisation, *Japanese Journal of Applied Physics*, Vol. 49, pp. 045102-1-6

Von Helden, G. et al. (1993). Carbon cluster cations with up to 84 atoms: structures, formation mechanism, and reactivity, *Journal of Physical Chemistry*, Vol. 97, pp. 8182-8192

Carbon Nanotubes - Synthesis, Characterization, Applications

Edited by Dr. Siva Yellampalli

ISBN 978-953-307-497-9
Hard cover, 514 pages
Publisher InTech
Published online 20, July, 2011
Published in print edition July, 2011

Carbon nanotubes are one of the most intriguing new materials with extraordinary properties being discovered in the last decade. The unique structure of carbon nanotubes provides nanotubes with extraordinary mechanical and electrical properties. The outstanding properties that these materials possess have opened new interesting researches areas in nanoscience and nanotechnology. Although nanotubes are very promising in a wide variety of fields, application of individual nanotubes for large scale production has been limited. The main roadblocks, which hinder its use, are limited understanding of its synthesis and electrical properties which lead to difficulty in structure control, existence of impurities, and poor processability. This book makes an attempt to provide indepth study and analysis of various synthesis methods, processing techniques and characterization of carbon nanotubes that will lead to the increased applications of carbon nanotubes.

InTech Europe
University Campus STeP Ri
Slavka Krautzeka 83/A
51000 Rijeka, Croatia
Phone: +385 (51) 770 447
Fax: +385 (51) 686 166
www.intechopen.com

InTech China
Unit 405, Office Block, Hotel Equatorial Shanghai
No.65, Yan An Road (West), Shanghai, 200040, China
中国上海市延安西路65号上海国际贵都大饭店办公楼405单元
Phone: +86-21-62489820
Fax: +86-21-62489821

IntechOpen